Chapter

The Magnetometry—A Primary Tool in the Prospection of Underground Water

Héctor López Loera

Abstract

One of the most important problems in arid and semi-arid zones in the Mexican Mesa Central is the one related to the exploration and exploitation of groundwater. It is found at depths over 200 m, and movement is primarily through fractures. This work presents a geophysical methodology, which shows the potential of combining natural and induced methods to locate confined aquifers in fault zones. The study begins by interpreting the aeromagnetic survey, mainly by searching alignments associated with low magnetic anomalies, which are correlated with faults zones, and/or fractures and/or geologic contacts where ferromagnetic minerals have undergone oxidation due to their association with recharged zones. These aeromagnetic alignments are confirmed on land by a ground magnetic survey. Based on these interpretations, electrical methods include sections and vertical electrical sounding are used to verify if the zones are correlated to the underground moisture. If both permeability and moisture are met together, then they considered as zones with a high probability of locating ground water in the Mexican Mesa Central.

Keywords: fractured-media aquifers, geophysical methods, aeromagnetics, semi-arid áreas, Mexican Mesa Central, San Luis Potosi

1. Introduction

Localization of ground water is a national and global issue at the priority basis. The fragility of water for various uses is a serious problem, which can be resolved by geological and Vertical Electric Soundings (VES) studies [1–3]. The problem arises when the geological information is not enough and accurate in the location of wells, resulting into dry wells. This problem is mostly frequent in volcanic areas, where the areas covered by alluvial material do not allow to observe the possible structures that contain underground water. In this study, we present a methodology for the location of this resource in arid volcanic zones, especially in the Central Mesa of Mexico. The methodology is based on a basic knowledge of Geology, the study of the magnetic field (air and ground) and the application of the electrical resistivity method, in two modalities, that is, sections and SEV [2].

The methodology was applied to solve serious water problem in the rural population of La Dulcita town, Municipality of Villa de Ramos, which is located at the Northwest of the capital of San Luis Potosí and state of Zacatecas (**Figure 1**). The population of La Dulcita in 2005 was reported with 750 inhabitants [4] and their water was supplied by a single well located at 5 km South of La Dulcita town, with

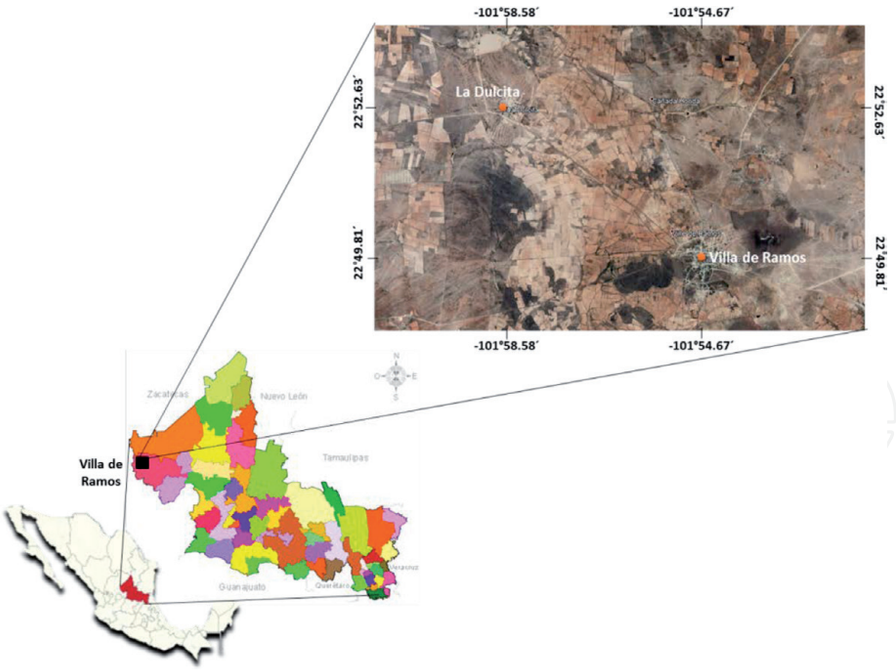

Figure 1.
Satellite image of study area, that is, La Dulcita, villa de Ramos, state of San Luis Potosí, Mexico.

its capacity measured less than 1 L/s, which was not sufficient for the entire population. In addition, the State Water Commission (CEA, for its acronym in Spanish), State of San Luis Potosí, had drilled three wells and all of them were dry.

The rocks that form the aquifers are characterized by their physical properties such as porosity, permeability and water content [5, 6]. The present methodology allows locating the zones and the degree of fracture and measure if these can be associated to moisture from the surface.

2. Study area

The Geology of the study area is represented mainly by the alluvial deposits approximately to the south of the La Dulcita, an outcrop of basaltic rocks exist in this area, whose height is approximately 15 m from the ground level (**Figure 2**). In the East, there are outcrops of the Caracol Formation, of the Upper Cretaceous [7] forming hills that protrude from the plains (**Figure 3**). It consists of shales of a greenish color, sometimes very dark gray. In the area of the Villa de Ramos, there is a large granite extension, which has almost a North-South course and constitutes a tectonic pillar that presents mineralization in some areas. In addition, also towards the North of Villa de Ramos, there are outcrops of marine sedimentary rocks [7].

La Dulcita area is located in a tectonic pit where the base must be represented by marine sedimentary rocks and probably basaltic lava flows.

3. Methodology

3.1 Geological survey

First, a compilation of the existing geological information that already exists of the State of San Luis Potosí that was published by the Institute of Geology, Autonomous University of San Luis Potosi and the Mexican Geological Service is performed. Once the existing information has been compiled, a geological survey

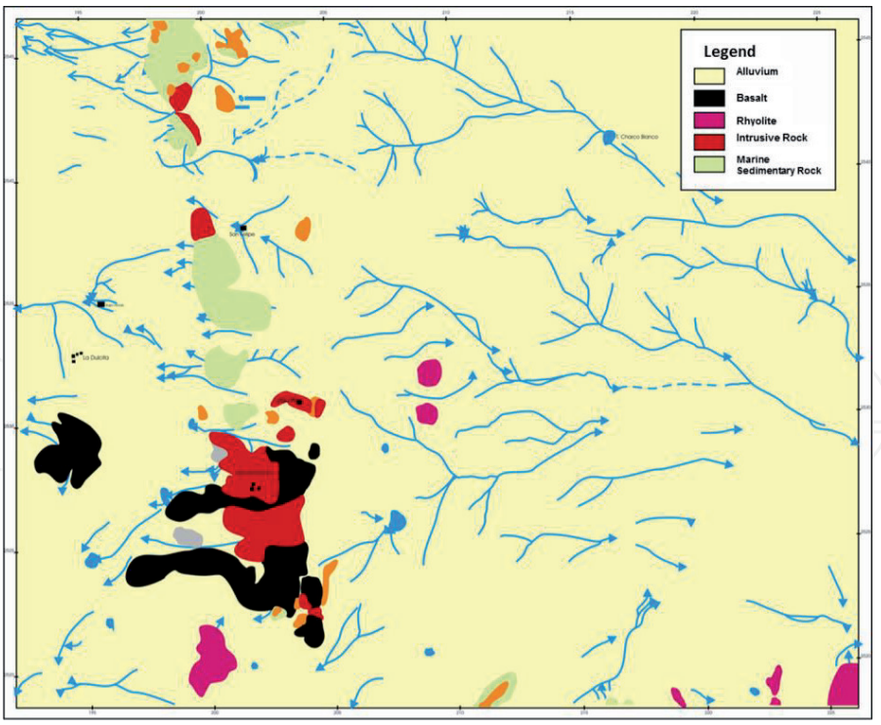

Figure 2.
Geological map of the Villa de Ramos area modified after Labarthe and Aguillón [7].

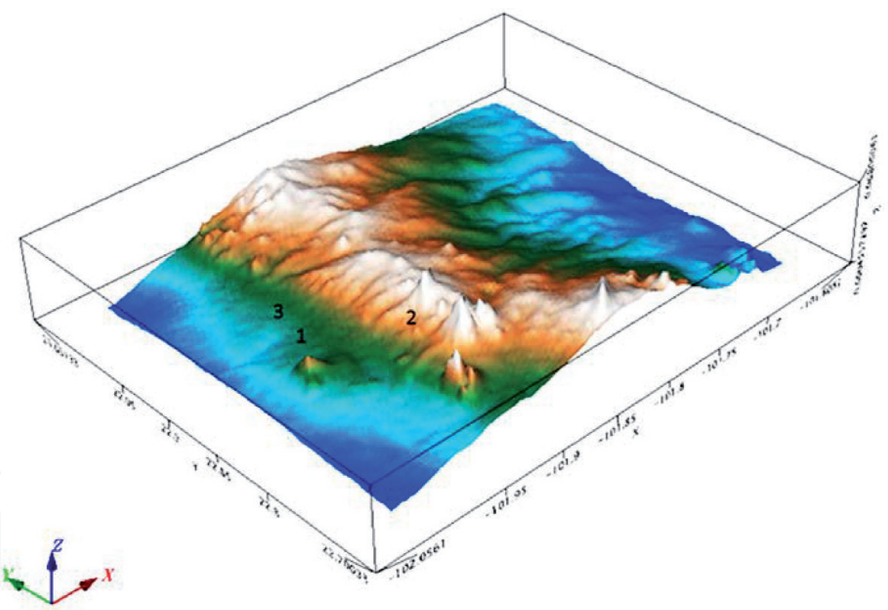

Figure 3.
Elevation digital model where La Dulcita (1) Villa de Ramos (2) and the H_2O well (3) are located, San Luis Potosí, Mexico.

of the study area is carried out to locate the geological units that can exist in the area under the study and a digital elevation model formed (**Figure 3**). In addition, **Figure 4** indicates a geological map of the study area and an idealized diagrammatic model where the main structures and existing geological units are indicated.

3.2 Geophysical study

The geophysical study is comprised of several stages; first, the aeromagnetic information of study area is analyzed. This is done by applying a series of mathematical algorithms (filters) to the aeromagnetic data, which allow highlighting certain

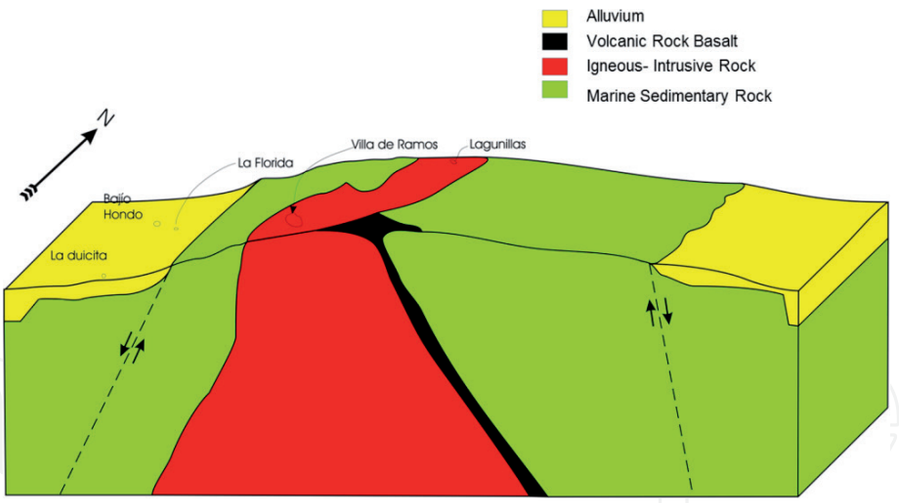

Figure 4.
Geological block of the La Dulcita-villa de Ramos area, San Luis Potosí, Mexico.

characteristics and dismiss others on the study area. The filters applied are known as International Geomagnetic Reference Field (IGRF) [8], which is calculated every 5 years and the immediate inferior should be applied to the date of the aerial survey (e.g., the aeromagnetic flight of our study area was carried out in 1995, the IGRF must be subtracted is that of 1990) [9]. To obtain the intensity values of the total magnetic field (TMF), which are obtained when flying, the contribution of the main dipole is subtracted, which exists in the terrestrial nucleus, thus obtaining the values of the residual magnetic field [RMF, Eq.(1)].

$$TMF - IGRF = RMF \quad (1)$$

Since the magnetic field is a vector (defined by magnitude and direction), the magnetic anomalies in these latitudes are displaced from the sources that produce them. Therefore, this is the reason why other mathematical algorithms must be applied for a filter, which simulates our study area, where the magnetic inclination is 90° and the declination is 0°. This algorithm named Baranov and Naudy [10] is better known as reduction to the magnetic pole field (RMPF) and assures us theoretically that magnetic anomalies will be located in the sources that produce them. The data matrix, thus generated, is the basis for the application of other filters or mathematical algorithms.

In arid volcanic areas, one of the opportunities to locate groundwater is in the confined aquifers on faults. A filter is a mathematical tool to guide us, if we want to know the fracture, faults or the contacts zones in the geological units a filter that provides us with guidance is the Henderson and Zietz [11]. This filter is known as vertical derivatives of first or second degree, because it is going to indicate the areas of high gradients which are normally associated with the geological structures mentioned above. Another filter that has been applied to aeromagnetic information is the Henderson [12] that allows us to change the plane of observation, when we rise, the high frequencies tend to attenuate and highlight the low frequencies, which are associated with the geological structure of the subsoil. This filter is known as the magnetic field upward continuation.

It is possible to interpret the location of the superficial and deep permeability zones with the analysis of the magnetic contour maps through each of these filters [13, 14].

The next step of the methodology, after the aeromagnetic information has been analyzed, is to perform a land magnetometry survey in the areas that have presented some possibility of being associated with fracturing and/or faulting and/or geological contacts [15, 16]. This stage is called anomaly verification.

The orientation of the land magnetic profiles should be as far as possible perpendicular to the structure that is inferred. The processing and analysis of the ground magnetic information is similar to the one made to the aeromagnetic data, a RMF is obtained from the TMF, later RMPF is generated and to this field, the filters of derivatives and upward continuation are applied.

The magnetic information analysis is up to a one-point simple. This method is based on the fact that the whole Earth behaves like a large magnet that would be in the center of it [17, 18]. For a specific area, it is considered that the magnetic field strength (**H**) is the same, and that the value of the magnetic intensity will be a function of the magnetic susceptibility of the rocks [*k*; Eq. (2)], which is defined as the capacity of these to acquire magnetization, such that:

$$\mathrm{I} = k\mathbf{H} \tag{2}$$

This magnetization (I) constitutes the induced magnetization. Additionally, the effects of the remnant magnetization are present. In volcanic and intrusive rocks, this magnetization can be of greater intensity than the induced effects [18, 19]. If we consider that volcanic rocks contain ferromagnesian and is without fractures, it will generate a magnetic response characterized by having an anomaly represented by a magnetic high and a low. That is, the magnetic response has a positive and a negative side. If we make the simile that the rock is a magnet, and fractured it in two parts, we would generate two anomalies, which would have two magnetic highs and lows in a sequence, high-low-high-low magnetic, and so on. If we have a slightly fractured and/or faulty area, it will give us a magnetic response with highs and lows sequenced, with medium frequencies. In contrast, if we have a zone with highly fractured and/or high faulting, it will give us a magnetic response characterized by high frequencies and by a series of sequenced of magnetic highs and lows [16]. These areas are interpreted as zones where two of three of the properties that identify the aquifers are present, as they have porosity and permeability.

Once the secondary permeability zone in the volcanic rocks has been identified, the next step in the methodology is to prove that the zones associated with humidity, which is achieved with the application of electrical methods; in our case, we use direct current.

The electric DC methods are based on Ohm's law [2], which establishes that the resistance is directly proportional to the voltage and inversely proportional to the intensity of the electric current:

$$R = \frac{\mathrm{V}}{\mathrm{I}} \tag{3}$$

where R (Ohm, Ω) is the electrical resistance, V (Volts) the potential and I (Amp) in the electric current.

The previous relationship (Eq. 3) is valid for any electrical circuit, in studies of the underground, the relationship changes since the resistance is a function of the nature and the geometry of the conductor (Eq. 4), in this case the Earth:

$$R = \frac{\rho \mathrm{L}}{\mathrm{S}}, \quad \rho = \frac{\mathrm{RS}}{\mathrm{L}} \tag{4}$$

The equation in which ρ represents the nature of the conductor and is called resistivity, L is the length in m and S the conductor section in m^2. If we replace and isolate the variable, then the following equation is given by:

$$\rho = \frac{\mathrm{VS}}{\mathrm{IL}} \tag{5}$$

In geoelectrical exploration, the resistivity of the underground is normally measured with an electrode arrangement of four electrodes, with the electrodes AB being the emission electrodes (current) and MN the potential electrodes.

In this case, the resistivity (Eq. 6) is given by:

$$\rho a = \frac{V}{I} \times 2\pi K \tag{6}$$

where K is the geometric factor (1/AM-1/BM-1/AN+1/BN) of the electrode array, the subscript "a" in the resistivity indicates that the calculated value is apparent.

The resistivity is an inverse property of the electrical conductivity and in exploration, its units is ohm per meter (Ω/m).

In geoelectric exploration, the variation of the resistivity is studied horizontally by means of profiles in which the electrode array is moved as a whole to the different stations. Conversely, equispaced or the vertical variation of the resistivity can be studied by means of vertical electric soundings (VES). At a certain point, for this, the current electrodes (AB) are increasingly opened and the measuring or potential electrodes (MN) are opened only when the measured values are very small (Schlumberger electrode array). In such manner in which data exist in one or two points with different MN opening for the same values of AB, there is an overlap or "cluth" during the measurement of the SEV [1].

A quick way to know the electrical behavior of the underground in a given area is to make profiles of electrical resistivity of two electrode openings, for example, at 200 and 400 m opening of the current electrodes with the Schlumberger electrode array (AB/2 at 100 and 200 m). In this way, we have knowledge of the variation of electrical resistivity in a horizontal direction.

If the resistivity behaves similar to both electrode array separations, it will imply that the entire electrically scanned area is the same. If the resistivity of the profile generated with a larger electrode aperture is higher than that generated at a smaller aperture, it will indicate that at depth the possibility of detecting humidity is zero. On the other hand, if the resistivity is lower at larger electrode aperture, it will have greater chances of detecting humidity. If the profiles of apparent resistivity show an irregular behavior, it will have greater possibilities of detecting a resistive resistance where the resistivity at the largest aperture changes form more resistive to less resistive and indicates that the area under study shows in the underground, where the current circulates more easily and will be an area where the variation of resistivity with depth must be studied, which is done with vertical electric sounding (SEV, [20]).

The VES' must be interpreted qualitatively and quantitatively. Firstly, the morphology of the VES curve must be defined [21] which in order to be associated with humidity, must necessarily have a correlation with the H-type curves ($\rho1 > \rho2 < \rho3$), which indicates that there is a lower resistivity contrast between the central layer and those that enclose it. The VES curves can also be KH ($\rho1 < \rho2 > \rho3 < \rho4$), QH ($\rho1 > \rho2 > \rho3 < \rho4$) or some of the curves that show a portion of type H.

The quantitative interpretation is carried out using commercial software that allows an inversion of the resistivity data [22]. It is convenient to perform a VES in wells where its stratigraphic column is known, in a way that the VES can be calibrated.

Once the previous stages have been carried out, the zones that are chosen for drilling must have a magnetic response which correlates with a fractured zone (permeability) and electrical methods (resistivity) with an area that has a relation with a humid area, represented by a resistive contrast that contains a minimum between two resistivity maxima.

4. Results

The procedure described above has been applied to an area, which is located in the Mesa Central, Mexico, specifically to a rural population called La Dulcita, municipality of Villa de Ramos, San Luis Potosí.

4.1 Air Magnetometry

The area under study was flown by the Mexican Geological Service, using an Islander aircraft BN2-A21, equipped with a Geometrics G-822 magnetometer, of cesium vapor optical pump, with a sensitivity of 0.25 nT, and an acquisition system of P-101 Picodas data, Automax video camera, 35 mm. A Geometrics G-826A magnetometer was used, with a sensitivity of 1 nT as the base station. Also, Sperry altimeter radar was also used.

The course of the flight lines was N-S, with a distance between flight lines of 1000 m and a height above ground level of 300 m, the navigation was controlled with an Ashtech GG24 GPS system and the data was subtracted from the IGRF 1990 reference.

The total magnetic field intensity in the central portion was 44,858 nT, with an inclination of 50°43′ and declination of 8°13′ for July 1995.

The magnetic field behavior analysis began with the generation of the RMF map (**Figure 5**), which as mentioned in previous paragraphs, is obtained by subtracting the IGRF from the total magnetic field. Based on the RMF, the RMPF was calculated (**Figure 6**). In the W portion of the RMPF, there is a "trend" of magnetic highs (red) that represent the W limit of an area of the graben that exists with a general direction N-S and is characterized on the map with anomalies associated with magnetic lows (blue color). Towards the central portion, two "trends" of magnetic anomalies with direction NE–SW and NNW–SSE are shown that are possibly associated with the geologically multiple intrusive "El Socorro" [7]. The Dulcita area is located on the first step of the graben and alignments (**Figure 7**) with direction N-S and E-W towards its portion W is observed, which can be geologically associated with zones of faults and/or fracturing and/or contacts. The area investigated in

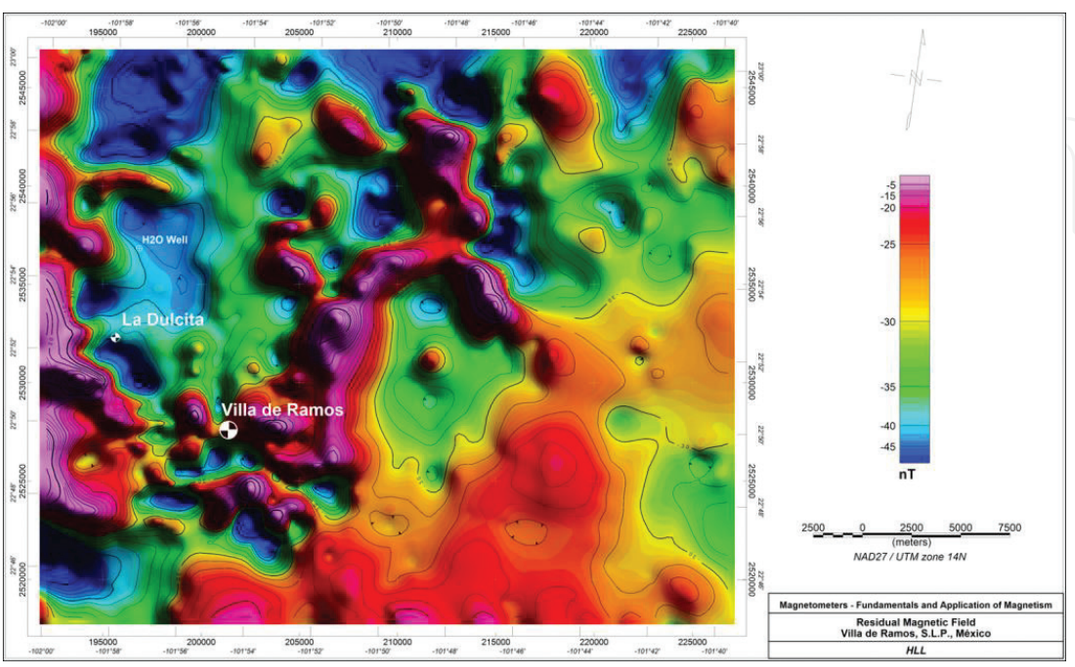

Figure 5.
Map showing the isovalues contour of the residual magnetic field of the Dulcita area, Villa de Ramos, San Luis Potosí, Mexico.

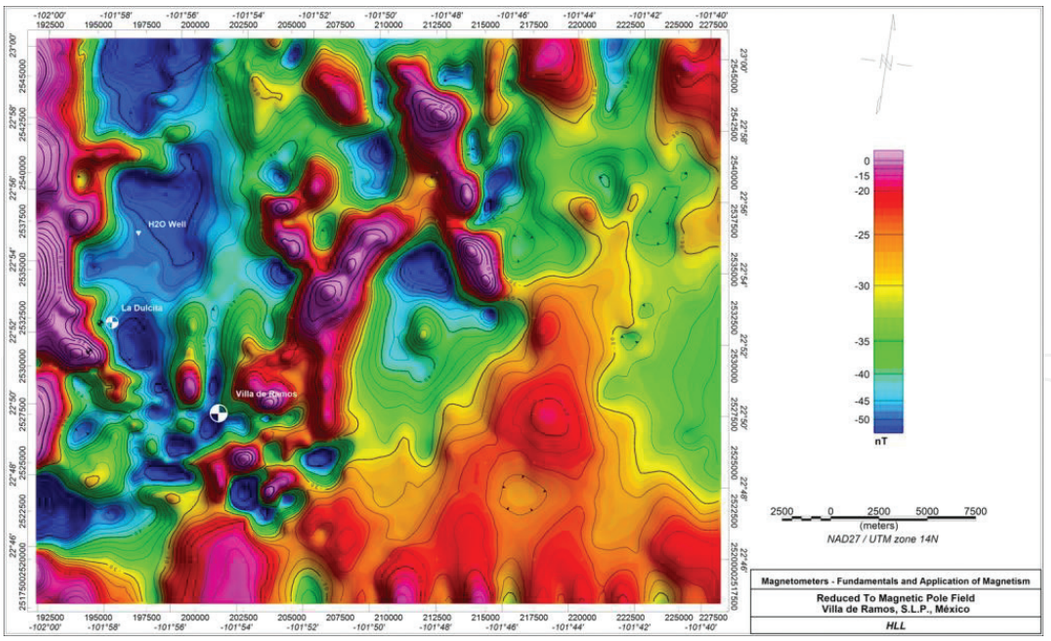

Figure 6.
Map showing the isovalues contour of the reduced to the pole magnetic field of La Dulcita, Villa de Ramos, San Luis Potosí, Mexico.

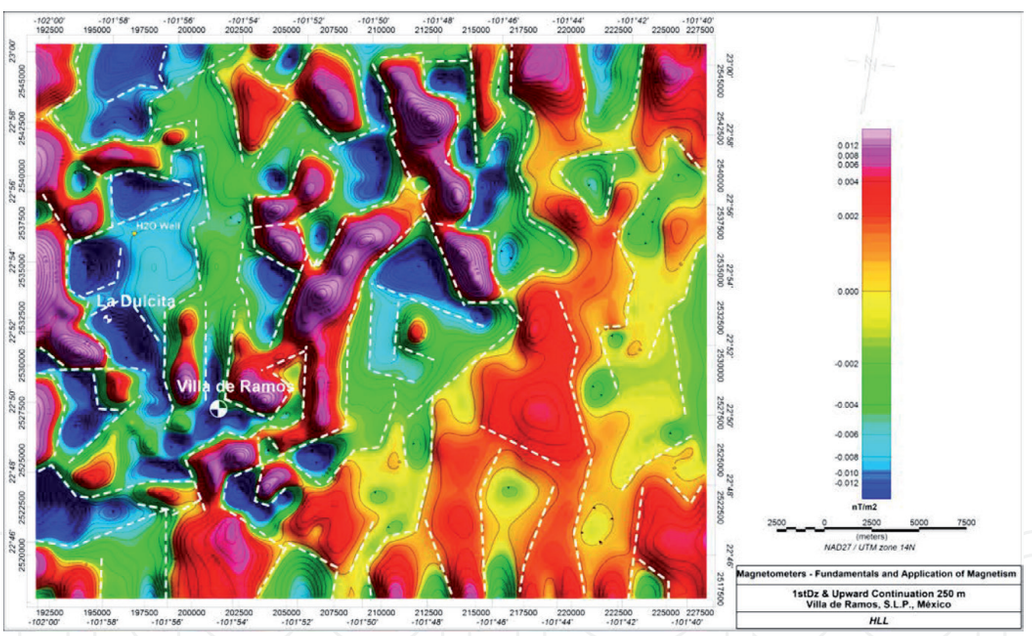

Figure 7.
Map where the magnetic alignments are observed based on the isovalues contour of the first vertical Derivativ upwards continuation 250 m from the reduced to the pole magnetic field.

general shows preferential aeromagnetic alignments in an N-S direction, also existing in the NE–SW direction, with few showing NW-SE direction.

The analyzed area in general shows the existence of up to 10 AMD's, each characterized by different amplitudes and wavelengths. The area where the water is extracted for the population of La Dulcita, is correlated with the AMD II that is associated with a tectonic pit area, characterized by low values of magnetism. The graben is limited by AMD I to W and by AMD's IIII and IV to the E. In AMD I, a highly productive well was located for the area (16 L/s) at a distance of 2.3 km SW of La Dulcita outside the ejido boundaries.

La Dulcita area is located in the aeromagnetic domain map (AMD), zone that show similar magnetic susceptibility (**Figure 8**) and is situated between the limits

of AMD's I, II and IX, which allows us to interpret possibilities of the existence of permeability in the zones of the contacts.

4.2 Ground Magnetometry

From above interpretation of the aeromagnetic information, four ground magnetic sections were programmed with reading stations of the total magnetic field (TMF), during every 20 m, by using two magnetometers, one GEM-GSM-19 and another Geometrics G-856 A, to perform the measurements, in which they were corrected by daily and hourly drift and a residual was obtained by subtracting a zero-degree polynomial from the TMF.

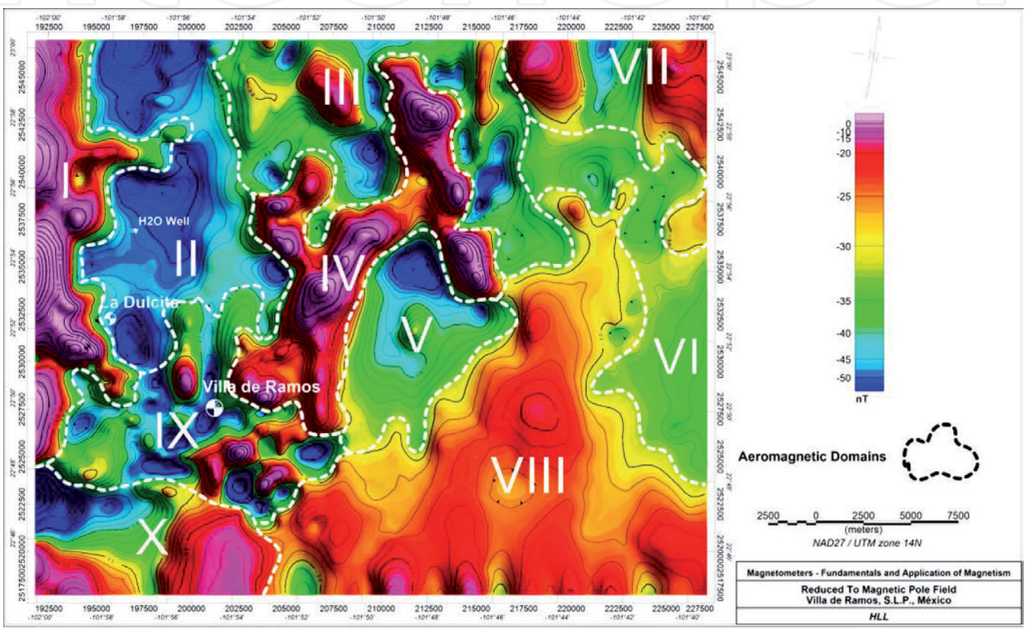

Figure 8.
Map of the aeromagnetic domains (AMDs) interpreted in the isovalues contour of the magnetic reduced pole field.

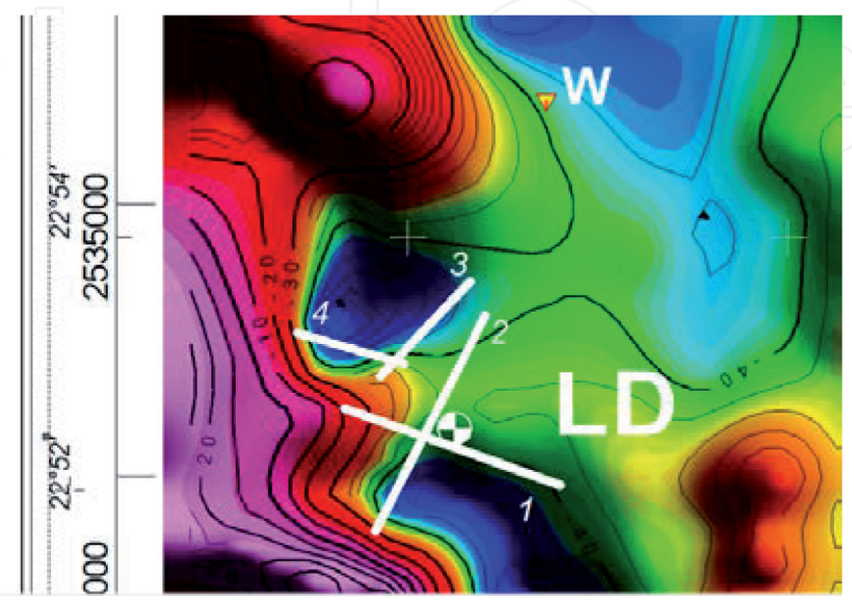

Figure 9.
Map showing the location of the ground magnetic sections. The water well that appears to the north of the map where the population of La Dulcita is supplied with a yield of less than 1 L/s.

Two of the sections had NW-SE orientation and two NE–SW (**Figure 9**) with the population of La Dulcita being in the central part of these profiles.

The magnetic section 1 (**Figure 10**) displays four terrestrial magnetic domains (TMD): first station 0 to 54 was characterized by a series of magnetic anomalies related to short wavelengths (20–40 m), high frequencies and amplitudes of 160 nT. It was geologically correlated with a highly fractured zone, while the horizontal gradients give values of up to 11 nT/m. Second, TMD 2 is located between stations 55 and 78, and it is defined by presenting a normal magnetic field, where no abnormal areas are observed. Third TMD 3 is located between stations 79 and 87 and shows an anomalous zone limited by two magnetic anomalies that have amplitudes of 33 and 65 nT and horizontal gradients of 2.6 and 6 nT/m, respectively. Geologically, it is correlated with an area of medium fracture possibilities. The last, TMD 4 is limited between stations 88 and 135, in general it shows a discretely disturbed magnetic field where it is not considered with the possibility of associating at depth with permeability.

The magnetic section 2 is located towards the E portion of La Dulcita (**Figure 9**), it presents five TMD's (**Figure 11**), the first one limited between stations 0 and 32 shows a normal behavior of the RMF, where magnetic anomalies are distinguished.

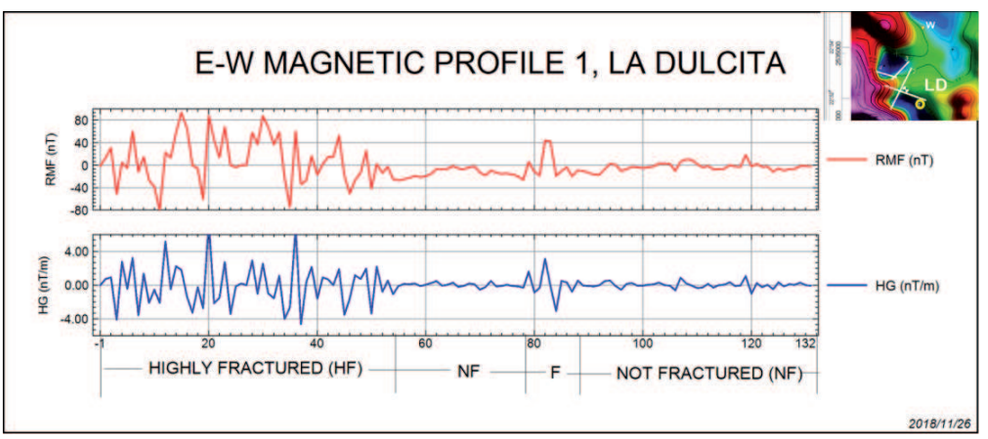

Figure 10.
Ground magnetic profile 1, with a NW-SE orientation. At the upper part, the residual magnetic field (RMF) is plotted (red); the horizontal gradient of the RMF is plotted at the lower part (blue), and at the bottom a qualitative interpretation of the percentage of probabilities of association with fracturing in the underground is shown. NF, not fractured; F, fractured.

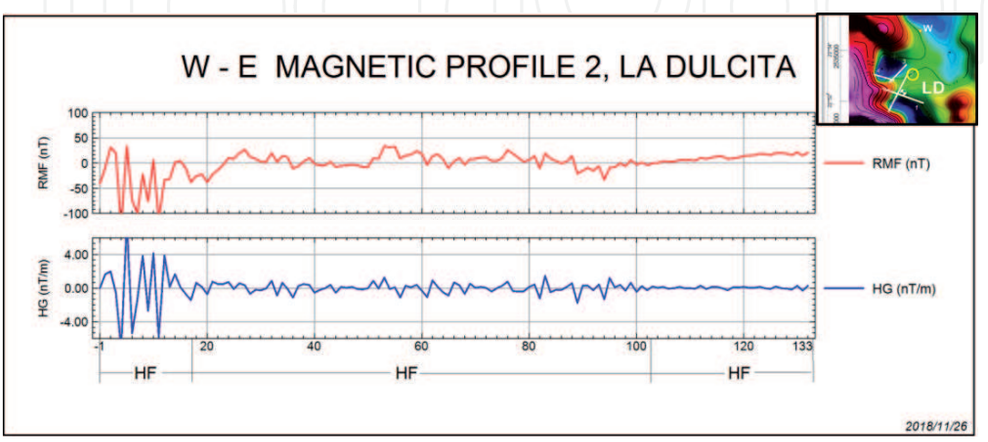

Figure 11.
Ground magnetic profile 2, with a NE–SW orientation. At the upper part the residual magnetic field (RMF) is plotted (red); the horizontal gradient of the RMF is plotted at the lower part (blue), and at the bottom a qualitative interpretation of the percentage of probabilities of association with fracturing in the underground is shown. HF, highly fractured; LF, light fractured; NF , not fractured.

The TMF 2 is located between stations 33 and 45 and does not show areas of high frequencies that can be correlated with fracturing effects at depth. The TMF 3 is located between stations 46 and 84, it is identified by presenting a magnetic response characterized by anomalies with short wavelengths (60–100 m), high frequencies and amplitudes of the order of 28–41 nT and horizontals gradients from 2.7 to 2.3 nT/m, respectively. It correlates an area with average possibilities that associating with the existence of secondary permeability. The TMD 4 is identified between stations 85 and 113 and has short wavelengths (20–80 m) high frequencies and amplitudes of 18 at 29 nT and horizontal gradients of 0.4–1.5 nT/m, respectively. They are geologically associated to an area with average possibilities of correlation with permeability in the underground. The TMD 5 is delimited between stations 114–133, characterized by showing short wavelengths (20–40 m), high frequencies and magnetization amplitudes of 54 nT up to 160 nT, with horizontal gradients of 6.5 nT/m up to 14.7 nT/m, is geologically correlated with an area of strong fracture and permeability.

The magnetic section 3 is located in the NW of La Dulcita (**Figure 9**) shows two TMD (**Figure 12**). The first domain is located between stations 1 and 16 is identified by presenting a series of magnetic anomalies. These are characterized by short wavelengths (20–100 m), high frequencies and amplitudes from 32 to 107 nT and horizontal gradients from 2.9 to 7.6 nT/m, which correlates with average possibilities of being associated in the underground with fracturing. The second TMD is located from station 17 to 75 and shows a normal magnetic field where the possibility to correlate with fracturing at depth zero.

The magnetic section 4 located outside La Dulcita, the NW portion (**Figure 9**), shows two TMD (**Figure 13**), neither of them of interest to be associated with fractured zones in the underground.

4.3 Electrical methods

Two electrical sections (or profiles) of apparent resistivity, induced polarization and self-potential were made with the Schlumberger type electrode array (**Figure 14**), using two electrode spacings AB/2 = 100 and 200 m and a Syscal R-2 resistivity instrumental (**Figure 15**). The sections were made in the same directions as the magnetic profiles 1 and 2, which were showed more possibilities of associating with fracturing in the underground.

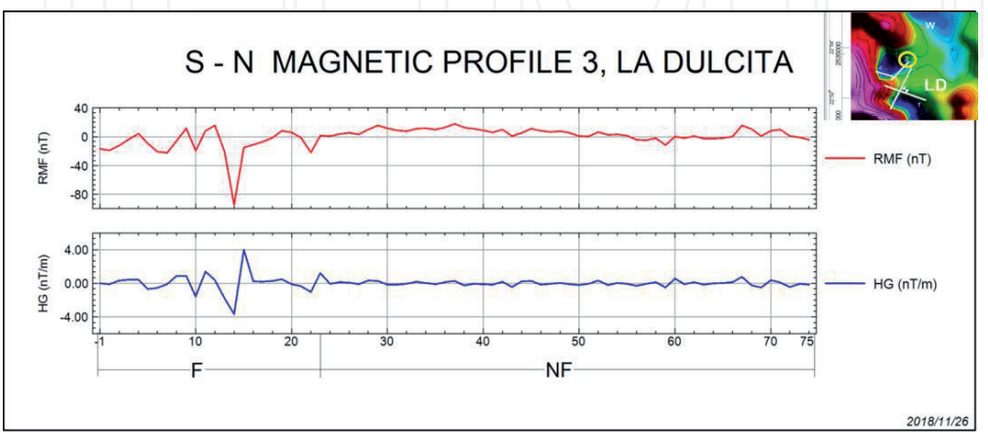

Figure 12.
Ground magnetic profile 3, with a NE–SW orientation. At the upper part the residual magnetic field (RMF) is plotted (red); the horizontal gradient of the RMF is plotted in the lower part (blue), and at the bottom qualitative interpretation of the percentage of probabilities of association with fracturing in the underground is shown. F, fractured; NF, not fractured.

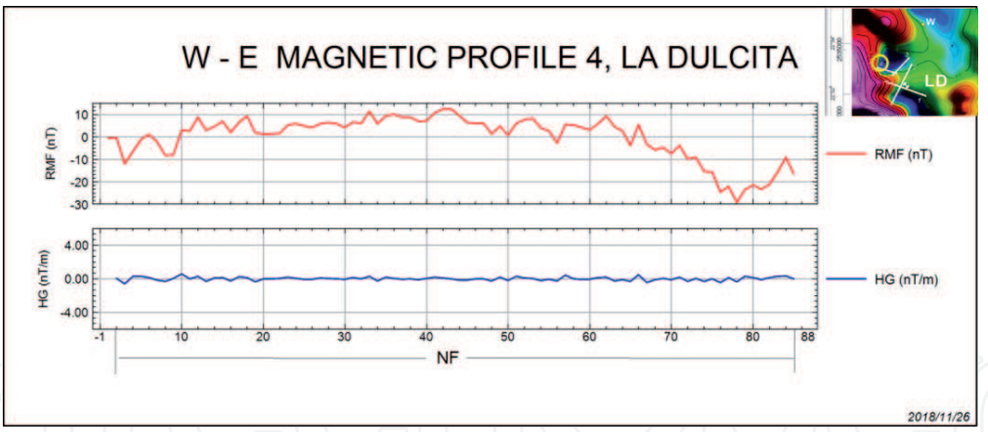

Figure 13.
Ground magnetic profile 4, with a NW-SE orientation. At the upper part the residual magnetic field (RMF) is plotted (red); the horizontal gradient of the RMF is plotted at the lower part and at the bottom a qualitative interpretation of the percentage of probabilities of association with fracturing in the underground is shown. NF, not fractured.

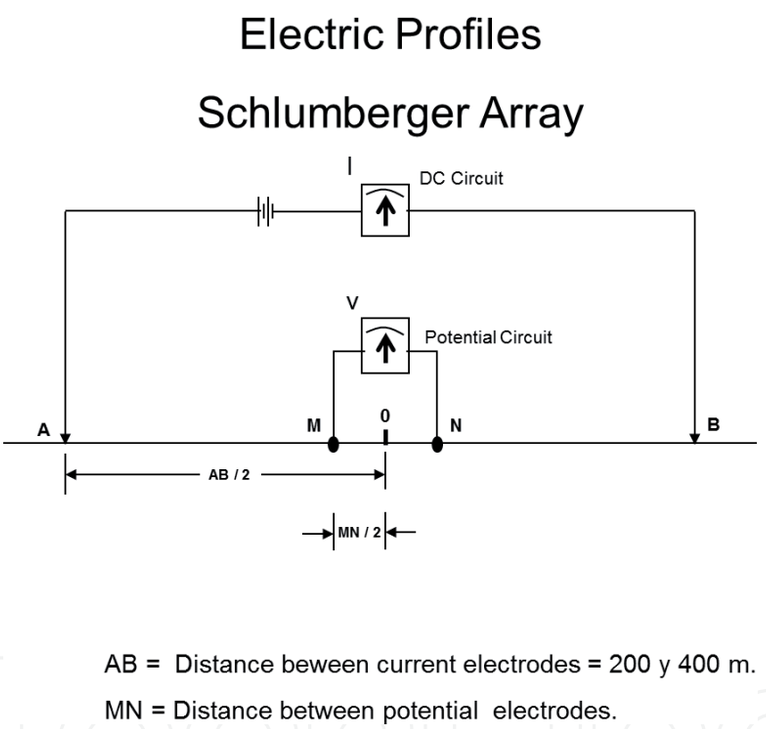

Figure 14.
The Schlumberger electrode array diagram, used for the realization of vertical electric sections and soundings (VES). The maximum openings of the VES were AB/2 of 1500 and 2000 m.

The W-E electrical profile shows in general an increase in resistivity with depth except two areas, from station 400 to 500 and 750 where the conductivity is higher. The induced polarization in these profiles generally shows a decrease in chargeability, except for two areas of station 450–500 and 750, where the load capacity tends to increase. The spontaneous potential is observed to decrease in general with larger separations of AB/2 (**Figure 16**).

The S-N electrical section, presents values of apparent resistivity lower at depth for the most part, except from station 450 to 550 where there is a small increase in resistivity to separations greater than AB/2. The chargeability values in the induced polarization are observed in contrast throughout the section, increase to greater separations of AB/2 in the areas of station 0–150, 350, 550–900 and in the station 1100. The spontaneous potential (SP) in this section behaves similarly to both

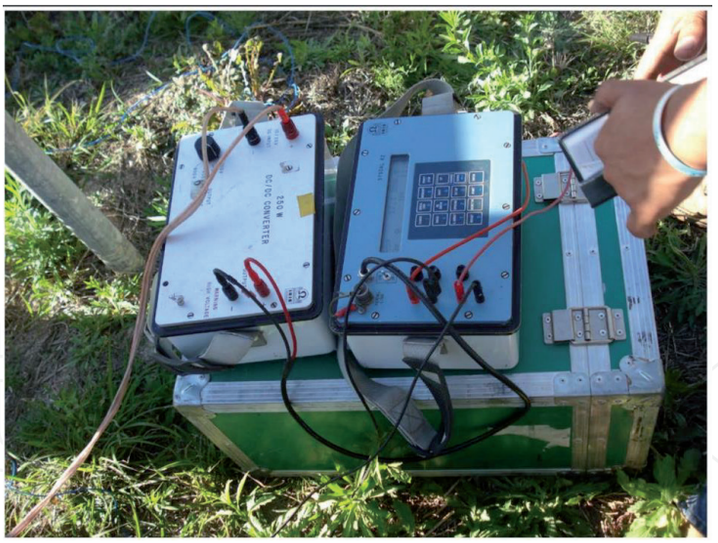

Figure 15.
Electrical instruments used for vertical electric soundings and sections.

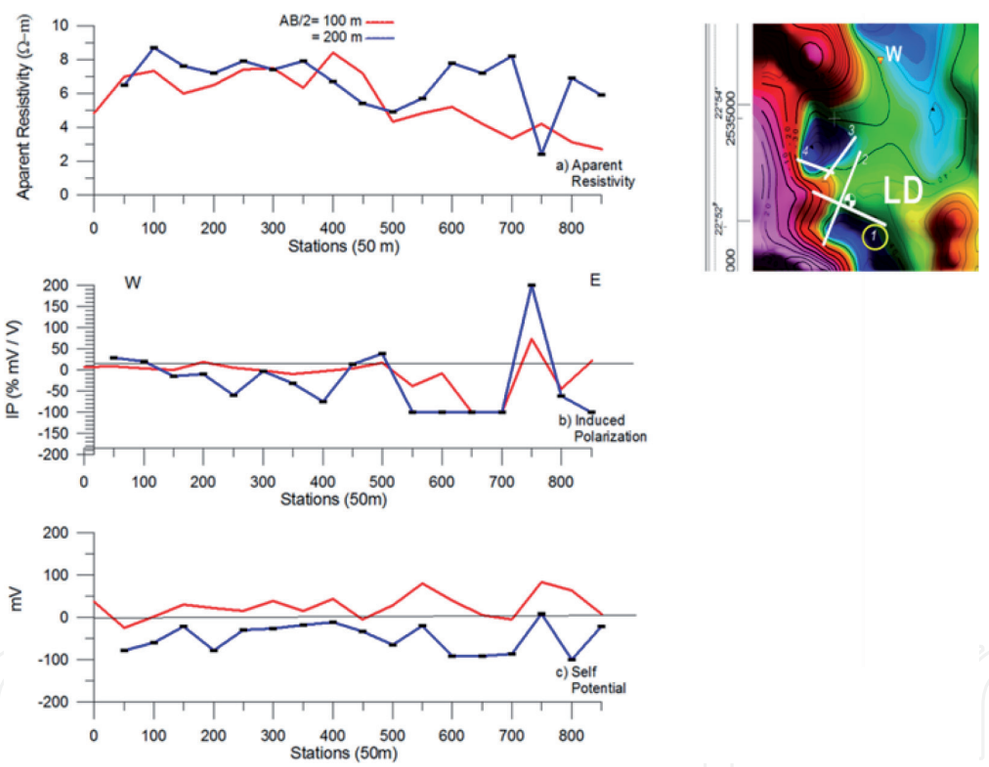

Figure 16.
Electrical profile 1, with a NW-SE orientation, where (a) the apparent resistivity is plotted; in (b) the induced polarization and in (c) the self-potential. These electrical profiles were located on the zones showing high frequencies (fracture, permeability) in profile 1 (Figure 10) of magnetometry.

electrode separations between stations 0 and 550, where at higher separations of AB/2, the values (mV) increase slightly from station 600 to 900, the values decrease for AB/2 = 200 m and from station 950 to 1300, the SP is changing (**Figure 17**).

4.3.1 Vertical electrical soundings

Five vertical electric soundings (VES') were made with maximum openings of the current electrodes (AB/2) of 1500 and 2000 m, four of them are located in identified zones (magnetometry) with possibilities of associating depth

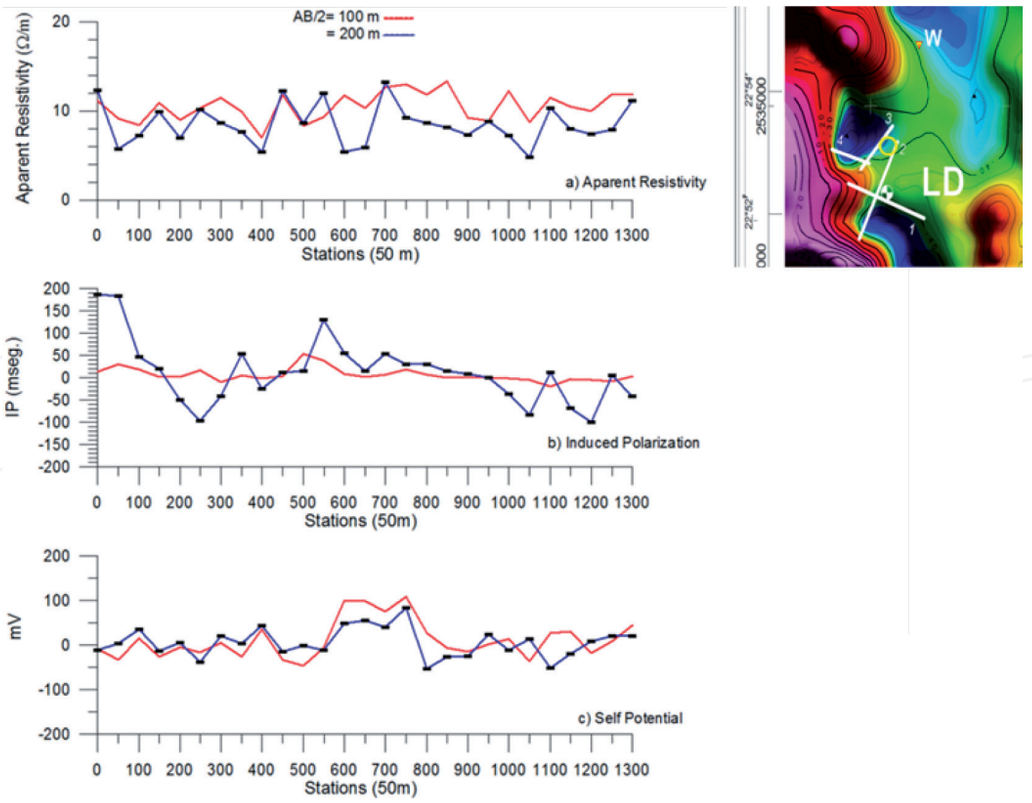

Figure 17.
Electrical section 2, with a NE–SW orientation, where (a) the apparent resistivity is plotted; in (b) the induced polarization and in (c) the self-potential. It is located on the magnetic section 2.

C#	RESISTIVITY	THICKNESS
	(ohm-m)	(meters)
1	205.7	2.47
2	3.21	21.25
3	23.23	33.54
4	6.68	398.9
5	3.06	163.0
6	43.66	

C#	RESISTIVITY	THICKNESS
	(ohm-m)	(meters)
1	64.78	2.70
2	101.1	37.47
3	28.69	170.4
4	2.02	157.8
5	10.84	

C#	RESISTIVITY	THICKNESS
	(ohm-m)	(meters)
1	102.4	2.44
2	18.65	30.25
3	9.11	167.6
4	6.32	674.8
5	81.10	

Figure 18.
Graphs of vertical electric soundings (VES) 1 and 2 and their comparison with VES 4, related to a well with an expenditure of the order of 25 L/s. note the thickness (170.4 m) correlated with the aquifer horizon (28.7 Ωm) possibly due to a sandy unit, overlying a clay horizon (2 Ωm).

permeability. One of the SEVs was carried out on a producer well that was located 2.3 km SW of La Dulcita and geologically located in the zone of the sunken block and aeromagnetically associated with the AMD I, which served as calibrator for the interpretations.

C#	RESISTIVITY	THICKNESS	C#	RESISTIVITY	THICKNESS	C#	RESISTIVITY	THICKNESS
	(ohm-m)	(meters)		(ohm-m)	(meters)		(ohm-m)	(meters)
1	53.78	3.35	1	64.78	2.70	1	684.6	4.50
2	4.45	58.09	2	101.1	37.47	2	48.89	11.11
3	53.20	34.22	3	28.69	170.4	3	14.81	29.08
4	3.48	228.0	4	2.02	157.8	4	9.24	719.1
5	55.22		5	10.84		5	27.06	

Figure 19.
Graphs of the vertical electric soundings (VES) 3 and 5 and its comparison with the VES 4, related to a well, with an yield of the order of 16 L/s. Note that VES 3 shows a sequence of geological units (~ 53 Ωm) confined by clay horizons (3–4 Ωm), while VES 5 shows a decrease in resistivity to depths of the order of 700 m.

The qualitative interpretation of the VES' morphology showed that the producer was well associated with a KQH curve (VES 4), among four remaining SEVs two were from the QQH family (VES 2 and 5), one was HKQH (VES 1) and the other HKH (VES 3).

The VES' were processed and interpreted with the commercial program Resix Plus that solves the inverse problem based on the Ghosh method of the inverse filter [22]. Each of the VES was compared with the VES (4) of the producing well (**Figures 18** and **19**).

Figure 18 indicates that the data interpreted in the VES 4 (KQH) for producing well and calibrator clearly indicates that at the base of the aquifer there is a clay unit (2 Ωm) and correlates with the resistivity of 28.69 Ωm with a thickness of 170.4 m, hence the well produces about 16 L/s. In this comparison, the VES 1 (HKQH) shows a horizon (23.23 Ωm) with a thickness of 33.5 m, possibly associating a sandy unit with moisture content at a depth of the order of 24 m. The VES 2 (QQH) shows a unit with a resistivity of 18.65 Ωm at a depth of less than 3 m with a thickness of 30 m.

Figure 19 shows the results of interpreting the VES' 3 and 5, they are also compared with the VES 4 (well). The VES 3 (HKH) shows the existence of a geological unit (53.20 Ωm) bordered by two clay horizons (4 and 3 Ωm) at a depth of the order of 61 m and a thickness of 34 m. It presents very good resistive contrast and the unit can be a fractured basalt horizon. VES 5 (QQH) shows a horizon possibly associated with a clay-sandy unit (14.8 Ωm) at a depth of 15 m and a thickness of 29 m. A large layer (> 700 m) of clay (9.2 Ωm) that starts to make an interpretation at a depth of 45 m.

5. Results and conclusions

Once the information was interpreted and analyzed, in some areas and communal land holding close to La Dulcita, a zone that meets the standards that are associated to the aquifer were found. It aeromagnetically shows the existence of alignments in N-S and E-W orientation and their location on top of the graben

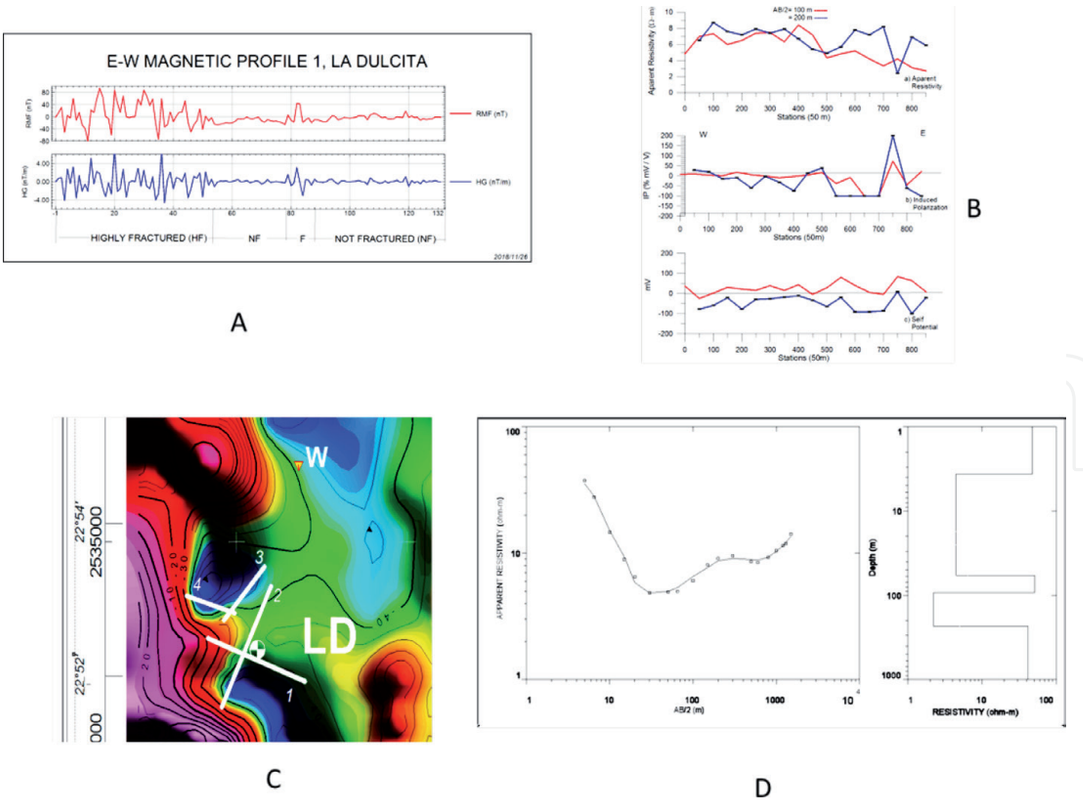

Figure 20.
The graphs that support the existence of a fractured area and with humidity in the underground are shown. The magnetism intensity graph (a) shows a clearly fractured zone towards the NW portion of the section. In the geoelectric profile (B), a contrast in resistivity is observed towards station 400, it decreases to openings of AB/2 = 200 m with respect to AB/2 = 100 m. the SEV 3 (C) shows association with type H curves.

structure. It is represented in an aeromagnetic map by the magnetic lows (blue color) the pit area and magnetic highs (color red). Thus, La Dulcita area is located in the limits of three aeromagnetic domains, which already indicates in ground magnetic measurements and should necessarily have a magnetic susceptibility contrast that will be reflected with significant differences in the amplitude of the magnetic field.

The ground magnetic sections indicate the zones that can be associated with permeability and the zones that do not have association with this physical property. The magnet simile is parameter for the interpretation of fracture in the underground. It will generate a simple anomaly if not related with fracture and provide a series of anomalies, which will be characterized by high frequencies. The calculation of the horizontal gradient of the magnetic field is completely resolutive to be able to observe fractured (permeable) zones of relatively healthy zones. In the magnetic section 1, the different physical behaviors that exist in the underground are clearly shown in the first portion of a highly fractured area contrasted with the rest of the section, which indicates that the magnetic susceptibilities of each terrestrial magnetic domains are associated with different units.

With the aerial and terrestrial magnetism, it was easy to find areas with high possibilities of being associated with fracturing (permeability).

With the electrical sections, it was possible to quickly scan the areas with possibilities of being associated with permeability and verify if they could also be associated with humidity. Producer well is key to facilitating the interpretation of vertical electric soundings, which in order to be associated with humidity should have as part of their morphology a portion type H.

In the area that was most likely to be associated with permeability and humidity in the underground (**Figure 20**) where a drilling was carried out by the State Water

Commission of San Luis Potosí, with production of 4 L/s. Furthermore, if we take into account the previously three dry wells, which had been drilled then it can be said that this methodology has met the objective.

With the help of the above methodology, the trained eye of the field geologist is strengthened with this methodology that uses scientific instruments, whose function is to detect the variation in the physical properties. For example, the magnetic susceptibility and resistivity of the rocks that are hidden below the Surface. Undoubtedly, the usage will certainly increase the percentage of successful drilled wells.

Acknowledgements

This work was funded by the State Water Commission, San Luis Potosí and COPOCYT-SLP. My sincere gratitude goes to Ing. Víctor J. Martínez Ruíz for his support to drawing geological map. I also thank David E. Torres Gaytán for his contribution in the preparation of this work. Also my sincere gratitude to Dr., Sanjeet Lumar Verna and Lucia Aldana Navarro for their comments on writing.

Author details

Héctor López Loera
Instituto Potosino de Investigación Científica y Tecnológica A.C. (IPICYT), Applied Geosciences Department, San Luis Potosí, México

*Address all correspondence to: hlopezl@ipicyt.edu.mx

References

[1] Keller GV, Frischknecht FC. Electrical Methods in Geophysical Prospecting. New York: Pergamos Press; 1966. 317 p

[2] Orellana E. Prospección Geoeléctrica en Corriente Continúa. Paraninfo: Bibloteca Técnica Philips; 1972. 523 p

[3] Kirch R. Groundwater Geophysics: A Tool for Hydrogeology. 2nd Edition: Springer; 2009. 548 p

[4] INEGI. 2010. Available at: http://www.inegi.org.mx/Sistemas/bise/mexicocifras/default.aspx?ent=24. (Accessed: July 2010)

[5] Freeze RA, Witherspoon PA. Theoretical analysis of regional groundwater flow, part 2. Effect of water-table configuration and subsurface permeability variations. Water Resources Research. 1967;**3**:623-634

[6] Tindall JA, Kunkel JR. Unsaturated Zone Hydrology for Environmental Scientists and Engineers. Boston MA: Prentice Hall; 1999. 625 p

[7] Labarthe HG, Aguillón RA. Cartografía Geológica 1:50,000, Hojas: Salinas y Villa de Ramos, Estados. De San Luis Potosí y Zacatecas. Folleto Técnico 106. Universidad Autónoma de San Luis Potosí, Instituto de Geología;1986. 52 p

[8] NOAA. 2010. Abilaable http://www.ngdc.noaa.gov/IAGA/vmod/igrf.html,

[9] Urrutia-Fucugauchi J, Campos-Enríquez JO. Geomagnetic secular variation in Central Mexico since 1923 AD and comparison with 1943-1990 IGRF models. Journal of Geomagnetism and Geoelectricity. 1993;**45**:243-249

[10] Baranov V, Naudy H. Numerical calculation of the formula of reduction to the magnetic pole. Geophysics. 1964;**29**:67-79

[11] Henderson RG, Zietz I. The computation of second vertical derivatives of geomagnetic fields. Geophysics. 1949;**14**:508-516

[12] Henderson RG. On the validity of the use of upward continuation integral for total magnetic intensity data. Geophysics. 1970;**35**:916-919

[13] Henkel H, Guzmán M. Magnetic features of fractures zones. Geoexploration. 1977;**5**:173-181

[14] López-Loer H, Urrutia-Fucugauchi J. Geophysical Study of Faulting Associated with the Colima Volcanic Complex: Volcan de Colima, Fifth International Meeting: Colima, Mexico, January 22-26, 1966, Abstract Volume. Colima: University of Colima; 1996

[15] Babu HVR, Rao NK, Kumar VV. Bedrock toporaphy from magnetic anomalies - an aid for groundwater exploration in hard- rocks terrains. Geophysics. 1991;**56**(07):1051-1054

[16] López-Loera H, Urrutia-Fucugauchi J, Alva Valdivia LM. Magnetic characteristic of fracture zones and constraints on the subsurface structure of the Colima volcanic complex, western México. Geosphere. 2010;**6**(1):35-46

[17] McElhinny MW. Paleomagnetism and Plate Tectonics. London: Cambridge Earth Science Series; 1973. 358 p

[18] Tarling DH. Paleomagnetism. Principles and Applications in Geology, Geophysics and Archaeology. Chapman and Hall Ltd; 1983. 379 p

[19] Urrutia-Fucugauchi J. Importancia del magnetismo remanente natural

en la interpretación de las anomalías magnéticas. Boletín Asociación Mexicana de Geofísicos De Exploración. 1977;**18**(4):83-116

[20] Iakubovskii IUV, Liajov LL. Exploración Eléctrica. Moscú: Editorial Reverté, S.A.; 1980. 421 p

[21] Orellana E, Mooney HM. Master Tables and Curves for Vertical Electrical Soundings. España: Interciencia; 1966. 125 p

[22] Ghosh DP. Inverse filter coefficients for the computation of apparent resistivity standard curves for a horizontal stratified earth. Geophysical Prospecting. 1971;**19**(4):769-775